Developing Ultra-microporous Metal Organic Frameworks for Selective Sorption of CO_2

Thesis submitted towards the partial fulfilment of BS-MS dual degree program

By

ANITA JUSTIN

20121106

Under the guidance of

Dr. R. Vaidhyanathan

Associate Professor

Department of Chemistry

Indian Institute of Science Education and Research

(IISER-Pune)

CERTIFICATE

This is to certify that the dissertation entitled "**Developing Ultra-microporous Metal Organic Frameworks for the Selective Sorption of CO_2**" has been submitted by Ms. Anita Justin (Reg. no: 20121106) at the Department of Chemistry, Indian Institute of Science Education and Research, Pune, towards the partial fulfilment of the requirements for the award of BS-MS dual degree during the academic year 2016-2017. This is the bonafide work of the student.

(R. VAIDHYANATHAN)

Date: 20th March 2017

Supervisor:
Dr. R. Vaidhyanathan,
Associate Professor,
Department of Chemistry,
IISER Pune.

Seal:

आर वैद्यनाथन/ R. Vaidhyanathan
सहायक प्राध्यापक/ Assistant Professor
भारतीय विज्ञान शिक्षा एवं अनुसंधान संस्थान
Indian Institute of Science Education & Research
पुणे / Pune - 411 008 India

DECLARATION

I hereby declare that the matter embodied in the report entitled "**Developing Ultra-microporous Metal Organic Frameworks for the Selective Sorption of CO_2**" are results of the work carried out by me at the Department of Chemistry, Indian Institute of Science Education and Research, Pune, under the supervision of Dr. R. Vaidhyanathan and the same has not been submitted elsewhere for any other degree.

Signature of student:

Date: 20th March 2017

Signature of supervisor:

Acknowledgement

It gives me immense pleasure to thank everyone who made this thesis possible. First and foremost I would like to thank my thesis supervisor Dr. R. Vaidhyanathan, for providing me an opportunity to pursue my master's project with him in his lab.

I would like to express my sincere gratitude to Prof. K.N. Ganesh for providing excellent research atmosphere and infrastructure.

I would like to thank my lab members Shalini, Dinesh, Rahul, Shyama, Debanjan, Aparna, Sattwickfor helping me in the lab. Especially, Shalini for her help with single crystal X-ray diffraction, adsorption experiments, data analysis and discussions. And, Rahul for his help with single crystal X-ray diffraction experiments, Dinesh, Shyama and Debanjan for their help with Adsorption instrument.

I would like to thank all my friends in IISER and outside for providing me comfort during the times of failures. I would like to thank all my school teachers for providing with basics.

Last but not the least, I would like to thank my parents, sisters, grandmother, especially my father and mother, because of them only I could come to IISER and be what I am right now.

~ Anita Justin

Contents

List of tables:

List of Figures:

Synopsis

CO_2 capture from flue gas is considered crucial because of CO_2 being a greenhouse gas contributing substantially to global warming. Currently, materials like aqueous amine solutions, zeolites, activated carbons are being used to capture CO_2 from large scale sources, but they require high regeneration energy and cost. Therefore, porous materials like Metal Organic Frameworks (MOFs) have recently attracted lot of attention mainly because of their tunable surface functionalities, pore size, low heat capacity etc. Very recently, for obtaining selective capture of specific gases ultra-microporous MOFs have been identified as a prime candidate. They are relatively cheap as they are formed from readily available small ligands. They are stable owing to small pores and limited void volumes. They offer high selectivity owing to their inherent molecular sieving ability and nano confined spaces lined with active functional groups. However, in many cases their capacities for gas molecules are not high. For example, for any useful CO_2 capture applications a capacity of well over 3 mmol/g at STP is required.

Statement of the problem: Developing ultra-microporous 3D MOFs with optimal capacity and selectivity for CO_2 over N_2, for application in post-combustion capture. In this project, we have developed MOFs employing rare-earth metals owing to their ability to adopt large coordination, which would result in three-dimensional cross-linked network. As another variation, we have investigated a Copper Isonicotinate MOFs with framework flexibility for low pressure CO_2 capture. In all cases, the ligands were chosen to be short and chelating to ensure ultra-microporous framework is formed.

Chapter 1

Introduction

Metal Organic Frameworks (MOFs) are organic inorganic hybrid materials, which are formed by self-assembly of organic linkers and metal nodes (metal ion, metal cluster) into an extended coordination network. They are easy to synthesize and possess high thermal and chemical stability. They can be highly porous and possess high surface area. It has been mentioned in the material of the month: Metal Organic Frameworks, that one pea sized gram of MOF material can host the equivalent surface area of 40 tennis courts. These characteristics of MOFs help in exploring its application in various fields like gas storage[1], gas separation[2], heterogeneous catalysis[3], proton conductivity[4], drug delivery[5], magnetism[6] etc. One of the main applications of MOFs which is studied widely is carbon dioxide (CO_2) capture from the flue gas. CO_2 is a major greenhouse gas which keeps the Earth's atmosphere warm. Rapid increase in population has led to increase in industrialization, deforestation, agricultural expansion, automobile productions etc. These anthropogenic activities have increased the global CO_2 emissions (80% worldwide) and in turn have caused increase in atmospheric temperature- global warming. According to NASA, the CO_2 concentration level reached 400 ppm in 2013, which was reported as the highest CO_2 concentration ever. According to United States Environmental Protection Agency (EPA), 76% of the greenhouse gas emission is CO_2 and 65% of it comes from fossil fuel burning and industrial process. Currently many materials are being used for the selective capture of CO_2 from the flue gas. Amine solutions are mainly used at the industrial processes for the selective capture of CO_2, where a nucleophilic attack on the amine by CO_2 forms a C-N bond to generate carbamate or bicarbonate depending on the amine solution. Solid materials such as zeolites and activated carbons are also employed as CO_2 capture sorbents because of their high porosity and surface area. Direct CO_2 capture from the atmosphere is quite difficult because of the dilution (0.039 mol %) compared to its capture form the exhaust of a power plant, in which its concentration is on average 12mol%[7]. Hence these capture materials are used at the power plant exhaust. Three main kinds of CO_2 capture methods have been suggested for their large scale capture from fossil fired plants: 1) pre-combustion capture done by de-carbonation of the fuel prior to combustion, 2) oxy-fuel combustion which is carried by re-

engineering the combustion process to produce carbon dioxide as a pure combustion product and 3) post-combustion capture i.e. separation of carbon dioxide from the products of combustion[7].

1.1CO_2 capture Materials

MOFs have been extensively investigated for their potential in capturing CO_2 from the flue gas- industrial effluent. About 65% of the emitted CO_2 is from the power plant exhaust generated by burning of fossil fuels. Such man-made emission is responsible for global warming, which is challenging the sustainability of life on Earth. The CO_2 occur at low partial pressures (15%) in these exhaust streams, with N_2 (75-85%) being the other predominant gas. Selective capture of CO_2 from this mixture is clearly a critical need.

Following materials are currently being used for CO_2 capture.

1.1.1 Aqueous alkanolamine solutions

Aqueous alkanolamine solutions are most widely used for selective CO_2 capture. But high regeneration energy used to break the C-N bond is a major drawback in these cases. The amine solution are also unstable towards heating, this limits the regeneration temperature for the complete regeneration of the material. Amine solutions decompose over time which decreases their performance over time. They are highly corrosive to the vessels hence the concentration has to be reduced to 40%. Most importantly the heat capacity of 40% amine solution to close to the heat capacity of water (C_p = 4.18 $JK^{-1}g^{-1}$) which represents more contribution to the regeneration cost[12].

1.1.2 Solid sorbents

Porous solid sorbents are used for CO_2 capture mainly because of its low heat capacity compared with aqueous amine solutions.

- **Zeolites**

Zeolites are porous aluminosilicates with extremely high thermal and chemical stability. They are widely studied for CO_2 capture from post combustion flue gas[13]. They come under microporous materials. For example, zeolites 13X, which has a relatively high surface area (SA_{BET} = 726 m^2/g) and pore volume (0.25 cm^3/g), display promising capacity for CO_2 at room temperature (16.4 wt% at 0.8 bar

pressure and 298K)[14, 15]. One of the problem with most of the zeolites is they can get easily saturated with water vapor in the flue gas steam, and, as a result adsorption of CO_2 decreases over time[16]. The enthalpy of adsorption of CO_2 for zeolites are much higher, hence high temperature is required for desorption of the captured CO_2[17]. Using the robustness of zeolites, the selectivity towards CO_2 can be enhanced by embedding charge balancing cations on the surface or in their pores. This is attributed to the high polarizing capability and quadruple moment of CO_2 over other flue gases like N_2, H_2 etc[10].

- **Activated Carbons**

Activated carbons are highly porous but amorphous materials, which are commonly prepared by pyrolysis of carbon containing resins, fly ash and biomass[18]. They do not have any strongly interacting adsorption sites for CO_2 especially at lower pressures, which is marked contrast with zeolites. Hence they have lower CO_2 capacity at low pressure. But their high surface area helps achieving higher CO_2 capacity at high pressure. For this reason, these materials are used for pre combustion CO_2 capture, where high pressure flue gas is produced. One of the studies revealed that the upper limit for CO_2 adsorption capacity within the activated carbons range from 10-11wt% in case of post-combustion CO_2 capture conditions and 60-70wt% in case of pre combustion CO_2 capture conditions[10]. Advantages of activated carbons over zeolites are, their hydrophobic nature which prevents saturation with water vapor and thereby no loss of working capacity over time[19]. Also due to low enthalpy of adsorption of CO_2, the regeneration temperature is very low compared to zeolites[19]. But the major disadvantage is the lack of crystallinity which hampers designed structure modeling.

- **Metal Organic Frameworks (MOFs)**

MOFs are promising materials for the selective adsorption of CO_2 from the flue gas because of their high porosity, high surface area, tunable chemical functionalities and robustness, thermal and chemical stability. A key advantageous feature is their high crystallinity; in most cases, they occur as single crystals whose structure can be solved to atomic-precision using X-ray crystallography. A crucial metric for high performance of materials for selective CO_2 capture is its enthalpy of adsorption. Enthalpy of adsorption of CO_2 is expressed as isosteric heat of adsorption (Q_{st}) as a function of quantity of CO_2 adsorbed[10].

First CO_2 adsorption study on MOF was performed in 1998 in MOF-2 (Zn(BDC)) by Omar Yaghi[20]. For the application of MOFs in real scenario, they should possess large CO_2 uptake at ambient temperature, selectivity towards CO_2 over N_2 and moisture. So far highest CO_2 uptake at room temperature and 35 bar pressure is for MOF-177 and MOF-200 with an uptake of 1470mg/g at 35 bar and 2437 mg/g at 50 bar respectively[21, 22].This practically means, a tank filled with MOF-177 would store 9 times more CO_2 and MOF-200 would store 17 times more compared to a same sized tank with no MOF[23]. Selectivity to CO_2 at relatively low partial pressure is most important because the post combustion flue gas has a high partial pressure of N_2 (0.75 bar) and low partial pressure of CO_2 (0.15 bar). CO_2/N_2 selectivity can be enhanced by decorating the pore surface with amines, strongly polarizing organic groups and exposed metal sites. In these cases CO_2 can be selectively adsorbed at lower pressure due to its high polarizing capability and quadruple moment[10].

Pore functionalized with nitrogen bases are widely studied for the selective CO_2 capture because of the interaction of quadruple moment of CO_2 with heteroatom in the framework, and also due to acid-base interaction between lone pair of nitrogen and CO_2. Ni-4-PyC MOF(IISERP-MOF2) made of isonicotinic acid possess very high CO_2 uptake at low pressure with high CO_2/N_2 selectivity of 1853 at 313K (composition of $14CO_2$:$86N_2$)[24].It is reported that MOFs made with amine functionalized organic ligands have higher uptake of CO_2 at low pressure compared to its isostructural analogue devoid of any such basic groups[25]. For example, in Zinc aminotriazolato Oxalate (ZnAtzOx) series the amine groups protrude into the pore and interact with the CO_2 leading to high and selective capture at low partial pressures.[26,27,28,29].The enhanced CO_2 adsorption is primarily due to the basicity of nitrogen donor atom, which in turn provides many polarizing sites.

Open metal sites provide a charge dense binding site for CO_2 owing to its quadruple and polarizing nature[10]. HKUST has a CO_2 uptake of 11.6wt% and N_2 uptake of 0.41wt% with selectivity of 101[31] and Q_{st} value of -29.9kJ/mol due the presence of open metal sites on activation[32]. M_2(dobdc) type(M =Mg, Mn, Fe, Co, Ni, Zn) MOFs are widely studied for selective CO_2capture at low pressure owing to the presence of open metal sites. The Mg_2(dobdc), reports a Q_{st} value of -46kJ/mol with selectivity ranging from 44 to 61[33,34].MIL-100, MIL-101 also exhibit open metal sites upon removal of coordinated water molecule upon activation.

Another challenge for CO_2 capture from flue gas is that MOFs should be stable towards moisture and steam in the flue gas. MOF-5 is so sensitive to moisture that even on mere exposure to humidity it loses its crystalline nature. It is reported that water hydrolyses the metal-ligand bond and breaks the framework in case of MOF-5 and IRMOFs[35]. The metal ligand bond strength can be increased either by using azolate based ligands[36]or by using high oxidation state metals like Cr^{3+}, Fe^{3+}, Al^{3+}, Zr^{4+}, Hf^{4+} instead of +2 state transition metals[10]. MIL series made of +3 oxidation state metals like Cr^{3+}, Al^{3+}, Fe^{3+} and UiO-66 series of MOFs made of Zr^{4+} are exceptionally water stable[37]. They form strong metal ligand bond because of hard acid hard base interaction.

Considering all this, most crucial parameter for the efficient performance of the CO_2 capture materials are selectivity toward CO_2 over other gases specially N_2. High affinity towards $CO_2$is required for optimal capacity at low partial pressures, but too strong an interaction with CO_2 is also undesirable because of the energy penalty in desorption of the captured material[10]. If the interactions are too weak, this would lead to very low selectivity of CO_2. Most importantly, the material should be highly stable under the condition of capture and regeneration so that it can be deployed industrially[10].

1.2 Design of MOF

The MOFs are designed on the basis of hard –soft acid base theory. Ligands are chosen in such a way that they form a strong coordination bond with the metal center and result in crystalline coordination framework. Most commonly used ligands are di, tri, tetra carboxylates and azolates, where oxygen of carboxylate and basic nitrogen of azolates forms strong coordination bond with the metal center. The oxygen of carboxylate groups behave as hard base and nitrogen atom in nitrogen based ligands behaves as intermediate base. Transition metals like Mn, Fe, Co, Cu, Zn, Ni which have an oxidation state +2 act as intermediate acids and can bind very strongly with both nitrogen functionality and carboxylate functionality. Whereas alkali metals, alkaline earth metals, lanthanides, transition metals in+3 oxidation state (eg., Y, Nb, Al) and +4 oxidation state (eg., Zr, Hf, Ti) come under strong acids and they bind efficiently with carboxylates of any linkers. But under high temperature and pressure conditions they can form coordinate bonds with nitrogen as well.

Careful choice of ligands can help us achieve the desired pore volume, surface area and selectivity towards a particular gas. Depending on the reaction conditions, metals form either metal ion or metal oxo clusters and the ligand bind to that cluster. In case of IRMOFs, zinc forms OZn_4 type oxo clusters, to which dicarboxylate ligands bind to form 3D porous frameworks[8]. The coordination of metal to ligand varies from 4 to 6 in case of transition metals and is 8 to 10 in case of lanthanides.

1.3Ultra-microporous MOFs for CO_2 separation

Ultra-Microporous MOFs are made of small ligands, which possess high stability and rigidity. The pore size ranges from 3 to 6Å and they do not have large surface area. They are highly stable towards moisture. They allow favorable CO_2-CO_2 interactions and large cooperative binding energies[26]. Ultra-micropores generated by a small ligand ensure hydrostatic and hydrolytic stabilities, stability towards humid gas streams and shelf life[38].Ultra-low parasitic energy of 655kJ/kg for post combustion CO_2 has been estimated in a Ni-4-PyC MOF(IISERP-MOF2), which is highly moisture stable and highly selective to CO_2/N_2 at 313K[24].A series of ultra-microporous Zn aminotriazolate oxalate MOFs are reported (fig. 1), with high selectivity towards CO_2/N_2 at room temperature with high surface area and heat of adsorption for CO_2 gas, where amine group is protruded into the pore, which in turn gives high interaction with CO_2 and thereby high heat of adsorption and high

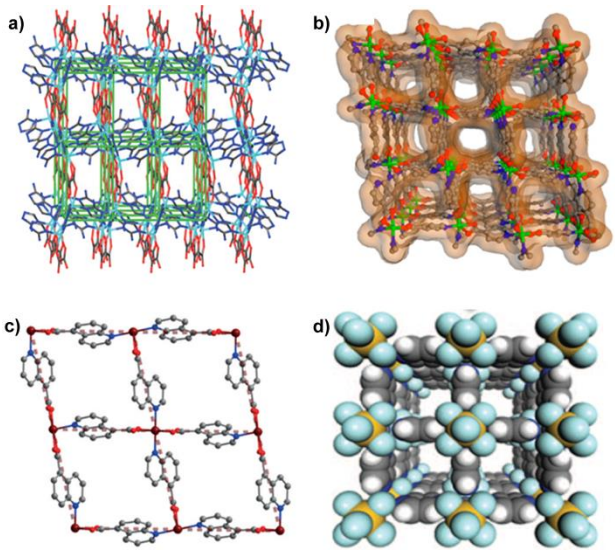

Figure 1: MOFs functionalized with basic nitrogen showing high CO_2 uptake and selectivity. Compounds: a) $Zn_2(Atz)_2(ox)$, b) IISERP-MOF2, c) Qc-5-Cu-sql, d) SIFSIX-3-Zn.

CO_2 capture at low pressure[26,27,28,29]. A series of [Cu(quinoline-5-carboxylate)$_2$]$_n$ MOFs and [Cu(4,4'-bipyridine)$_2$(SiF_6)]$_n$(SIFSIX) MOFs are developed, which are ultra-microporous and possess very high selectivity towards CO_2/N_2 and CO_2/CH_4[2]

1.4 Aim of the thesis

Thesis titled, 'Developing Ultra-microporous Metal Organic Frameworks for Selective Sorption of CO_2' focuses on constructing Yttrium based novel MOFs utilizing some of the readily available small molecules as ligands (Oxalic Acid and Fumaric Acid). The high charge and coordination numbers of the rare earth cation should facilitate the incorporation of high density of ligands in the framework, which can be anticipated to form a highly cross-linked 3D structure capable of forming ultra-micro pores with high separation capabilities and the strong covalent linking should ensure thermal and chemical stability. As a separate target, based on our prior success with Nickel isonicotinates, we have tried to develop a copper isonicotinate MOF for CO_2 separation application. As already mentioned in the introduction, the selectivity towards CO_2 over N_2 can be attained by using nitrogen functionalized basic ligands. Isonicotinic acid (INA) is one such ligand. Nitrogen of INA can bind efficiently with transition metals with +2 oxidation state. Prior literature reports indicate that Cu(INA)$_2$ MOF has been prepared before and has been found to be robust, particularly exhibits stability towards water[39]. Interestingly, the framework is responsive to solvent adsorption[6]. However, only their magnetic properties have been explored[41]. Our aim is to optimize the adsorption properties of this MOF for selective CO_2 capture, by tuning the framework via solvent templation. We have employed a range of alcohols for this purpose from MeOH, EtOH to PrOH. The Cu(INA)$_2$ MOF has been probed via gas adsorption studies and its surface area, pore volume, pore width and isosteric heat of adsorption (Q_{st}) and most importantly CO_2/N_2 selectivity have all been estimated.

Chapter 2

Research Methods and Instruments

2.1 Materials and Synthesis Methods

2.1.1 Chemicals

Copper chloride dihydrate ($CuCl_2.2H_2O$), Yttrium nitrate hexahydrate ($Y(NO_3)_3.6H_2O$), Isonicotinic acid (HINA,$C_5H_4O_2N$), Oxalic acid ($C_2O_4H_2$), Fumaric acid ($C_4H_4O_4$) were bought from Sigma Aldrich and used as such without further purification. Solvents used were N,N'-dimethylformamide (DMF), Methanol, Ethanol, Propanol and Distilled water.

2.1.2 Hydrothermal/Solvothermal Synthesis

Throughout this project, MOFs were synthesized by this method. In this method, the reactants were mixed with the solvent and placed in a Teflon liner. The Teflon liner was sealed inside a steel jacket. The autoclave was heated to a desired temperature and held at that temperature for several hours to days and then cooled down to room temperature slowly. Crystallization happens under high temperature and autogenous pressures. For reactions below 120°C, scintillation vials were also used. They also perform the same function as autoclaves do.

2.2 Instrumentation:

2.2.1 Single Crystal X-Ray Diffraction

Single-crystal data was collected on a Bruker SMART APEX four-circle diffractometer equipped with a CMOS photon 100 detector (Bruker Systems Inc.) and with a Cu Kα radiation (1.5418Å). The incident X-ray beam was focused and monochromated using Micro focus (IµS). Crystals were mounted on nylon Cryo loops with Paratone-N oil. Data was collected at 100 K. Data was integrated using Bruker SAINT Software and was corrected for absorption using SADABS. Structure was solved by Intrinsic Phasing module of the Direct methods and refined using the SHELXTL2014 software suite. All non-hydrogen atoms were located from iterative examination of difference F_{maps} following which the structure was refined using least-squares method. Hydrogen atoms were placed geometrically riding mode.

2.2.2 Powder X-Ray Diffraction

Powder XRDs were carried out using a Rigaku Miniflex-600 instrument and processed using PDXL2software.

2.2.3 Thermogravimetric Analysis (TGA)

Thermogravimetry was carried out on NETSZCH TGA-DSC system. The TGAs were done under N_2 gas flow (20ml/min) (purge + protective) and samples were heated from RT to 550°C at 4K/min.

2.2.4 Adsorption Instrument

Adsorption experiments are performed on **micromeritics ASAP 2020** and **Quantachrome-IQ** instruments, using ultra high purity grade gases. About 100mg of sample was transferred to the analysis tube and then evacuated (10^{-6} mbar) at which point the outgas rate was ≤ 2 µbar/min.

2.3 Theories on Adsorption

2.3.1 Adsorption Isotherms

Adsorption isotherms are simply a measure of the molar quantity of gas taken up or released, at a constant temperature T by an initially clean solid surface as function of pressure[41]. The gas before being adsorbed is called the adsorptive prior to adsorption and as the adsorbate after being adsorbed. Adsorption increases with increase in pressure and decrease in temperature. It is an exothermic process. Surface area and pore volume can be obtained from adsorption isotherms.

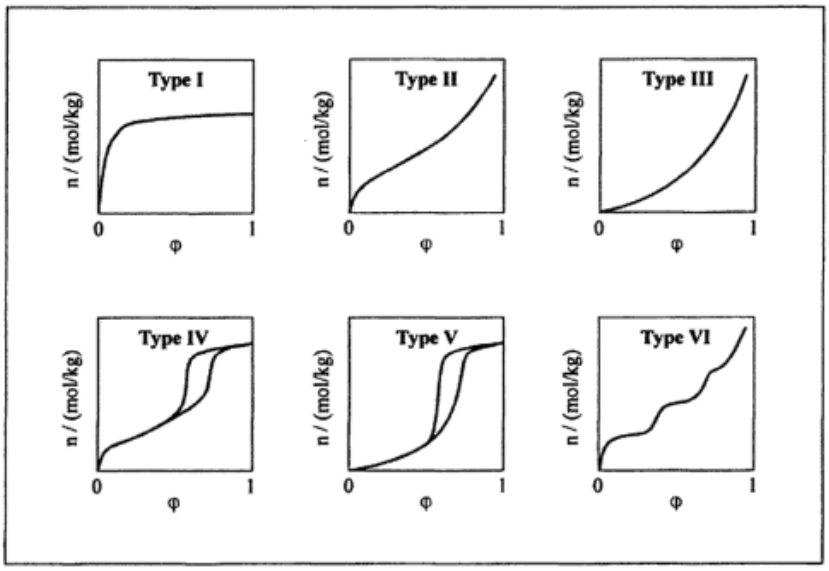

Figure 2: IUPAC classification of adsorption isotherms[43].

n= quantity adsorbed

$\phi = P/P_0$ (relative pressure).

Type I: corresponds to microporous adsorbents, where n reaches a saturation point when P/P_0 tend to 1 (fig 2).

Type II: corresponds to non-porous and macroporous adsorbents, with unrestricted monolayer-multilayer formation.

Type III: isotherm is convex to ϕ axis, indicating strong adsorbate-adsorbate interactions.

Type IV: corresponds to mesoporous adsorbents, where the presence of hysteresis loop indicates the capillary condensation in mesopores. Loading n approaches a limit as $\phi \rightarrow 1$.

Type V: Similar to type VI isotherm except that the initial part of the isotherm indicate weak adsorbate-adsorbate interaction.

Type VI: corresponds to step wise multilayer adsorption on a uniform non-porous adsorbent.

2.3.2 Langmuir Isotherm Theory

This theory was proposed by Langmuir in 1918. The model assumptions are

- Gas molecules behave ideally.
- Each adsorbate molecule occupies a single site.
- The surface is energetically homogenized.
- Adsorbed molecules are immobilized to the local site.
- Only one monolayer forms

The well known Langmuir isotherm formula is given below

$$\theta = \frac{KP}{1 + KP}$$

$\theta$is the fractional coverage expressed as $\theta = n/n_m$

n_m is the monolayer capacity of the adsorbent.

K is the equilibrium constant expressed as $K = \frac{\theta}{[(1-\theta)P]}$

At low pressure region (KP<<1), Langmuir equation reduces to Henry isotherm[43]

$$\theta = KP \text{ or } n = HP$$

H is Henry coefficient. From Langmuir equation, Henry coefficient can be calculated,

$$H = K\, n_m$$

At high pressures (KP>>1), θ reaches 1 and loading n approaches monolayer coverage n_m. Loading decreases with increase in temperature, hence K become smaller at higher temperature. Parameter K generally gives the type of adsorbate located on the surface.

Langmuir isotherm is expressed in linear form as given below

$$\left(\frac{P}{W}\right) = \left(\frac{1}{Wmb}\right) + \left(\frac{P}{Wm}\right)$$

Wm is the quantity adsorbed for the monolayer formation, b is an empirical constant.

Specific surface area is given by the equation,

$$S = \frac{Wm\sigma Na}{mVo}$$

N_a is Avogadro number, σ is surface area occupied by a single gas molecule, m is mass of the adsorbent, V_0 is the volume at STP.

2.3.3 BET Isotherm Theory

BET adsorption isotherms are also base on some assumptions like,

- Gases behave ideally
- Multiple gas molecules can be adsorbed at each site.
- Multilayer formation.
- Adsorbed molecules are immobile.
- No adsorbate-adsorbate interaction.
- Adsorbent is energetically homogenized.

BET isotherm equation is $W = \frac{WmCP}{(Po-P)*[(C-1)\left(\frac{P}{Po}\right)+1]}$

C is the equilibrium constant.

In linear form, the equation is represented as below

$$\frac{1}{\left[W\left(\frac{Po}{P}\right)-1\right]} = \frac{1}{WmC} + \frac{C-1}{WmC}\left(\frac{P}{Po}\right)$$

Values of C and W_m are obtained from the linear plot.

The surface area is calculated by the equation,

$$S_{BET} = W_m \sigma N_a$$

W_m is quantity required for monolayer formation, σ is the cross sectional area of adsorbate, N_a is the Avogadro number.

Chapter 3

Synthesis and characterization of three-dimensionally cross-linked MOFs with high oxidation state metal and small dicarboxylate ligands: case study Yttrium.

3.1 Synthesis

3.1.1 Synthesis of Yttrium oxalate $Y_2(C_2O_4)_3(H_2O)_2\bullet(H_2O)_4$ *(**1**)*

1 was synthesized hydrothermally, by heating 1mmol of $Y(NO_3)_3\bullet 6H_2O$, 1mmol of fumaric acid and 0.5 mmol of oxalic acid in 10ml water in a 20 ml autoclave at 150°C for 48hrs followed by slow cooling to room temperature (over 12hrs). Thin rod shaped colourless crystals were filtered and washed with water, methanol and air dried. The total yield of the reaction was121 mg.(Only oxalate binds to the metal center to form an extended structure)

3.1.2 Synthesis of Yttrium fumarate $Y_2(C_4H_2O_4)_3(H_2O)_2\bullet(DMF)_2$(**2**)

2 was synthesized solvothermally, by heating 1mmol of $Y(NO_3)_3\bullet 6H_2O$, 1 mmol of fumaric acid in 1:1 mixture of DMF and distilled water in a 12ml scintillation vial at 90°C for 24 hrs followed by slow cooling to room temperature over a period of 12 hrs. Plate shaped colorless crystals were filtered and washed with water, methanol and air dried. The total yield of the reaction is 207 mg.

3.2 Result and Discussion

3.2.1 Single crystal description of 1

Table 1: Crystal description of 1.

Empirical formula	$Y_2(C_2O_4)_3(H_2O)_2\bullet(H_2O)_4$
Formula weight (g/mol)	549.96
Crystal system	Trigonal
Space group	$\bar{R}3$
Unit cell length (Å)	a= b= 30.58, c= 7.06
Unit cell angles	α= 90°, β= 120°,γ= 90°
Volume	5729Å^3

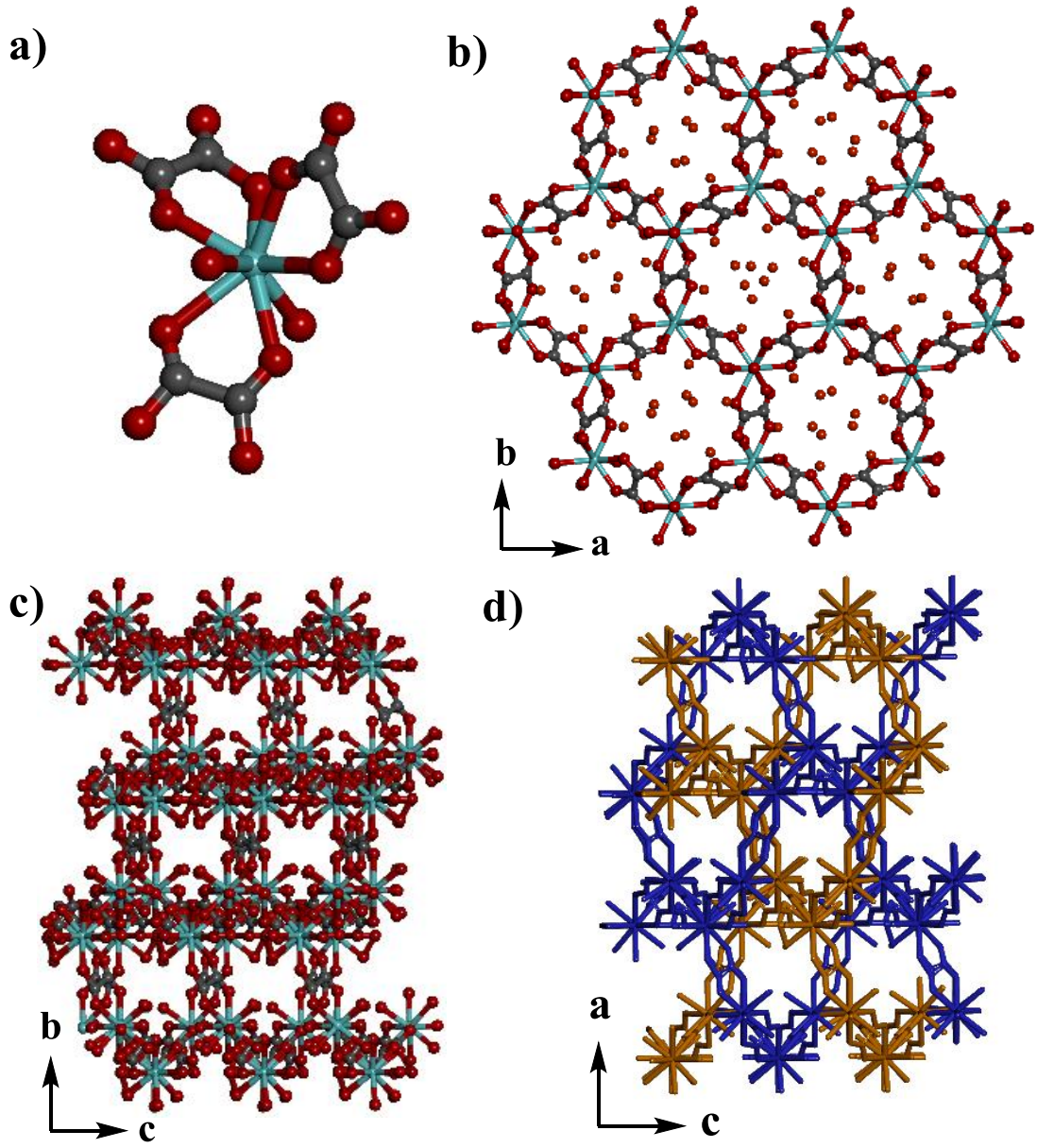

Figure3:Single crystal structure for **1.** a) represents coordination sphere of Yttrium. crystal structure view along b) c-axis, c) a-axis, d) b-axis (solvents along a and b axishave been removed for clarity), showing interpenetration [Color scheme: Orange-sky blue, Grey- Carbon, Red-Oxygen]

Yttrium atom in **1** has 8 coordinations satisfied by three oxalate moieties and two water molecules (fig 3a). The metal centers are connected by oxalates to form hexagonal shaped channels along c-axis (fig 3b).The structure is porous along all three axes (fig 3b, 3c, 3d). Figure 3(d) shows that the framework is not an extended 3D network, but instead two 2D layers interpenetrated to form 3D structure. The interpenetration could reduce the accessible void volume. PLATON software reveals a void volume of 39% for the squeezed framework.

3.2.2 Bulk Characterization of 1

Bulk characterization was done using PXRD and TGA.

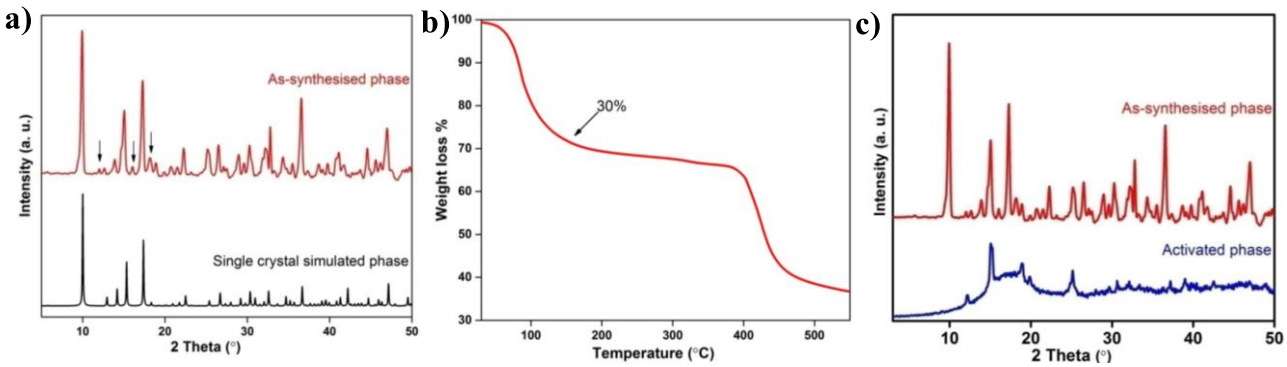

Figure 4: Bulk characterization: a) PXRD of bulk and SC simulated of **1**, b) TGA of **1**, c) PXRD of **1** after activation at 140°C.

PXRD comparison of as-synthesised and single crystal simulated XRD reveals that the phase is not completely pure as we see two low intensity peaks at 11.9° and 16.02°. This might be due to presence of fumaric acid used in the reaction. Therefore, we tried synthesizing **1** without the fumaric acid. Unfortunately, it resulted in a known phase. TGA shows a weight loss of approximately 30% from 30°C to 200°C. This 30% weight loss could be attributed to the removal of water from the pore

.**1** is stable up to 400°C. Our main focus is to access the 39% void volume for CO_2 capture. The activation of sample is at 140°C for 6hrs under vacuum of 10^{-5} torr resulted in the framework collapse, which is identified from the PXRD of activated sample. Even simply heating at 80°C resulted in the framework collapse. This can be due to the strong hydrogen bonding interaction between the pore water molecules among themselves and with the framework. This is an example of first generation MOF[43].

In our attempts to avoid the hydrogen bonding in **1**, we used DMF/H_2O mixture as solvent instead of water and used only fumaric acid ligand and ended up with **2**.

3.2.3 Single crystal description of 2

Table 2: Single crystal description of 2

Empirical formula	$Y_2(C_4H_2O_4)_3(H_2O)_2.2DMF$
Formula weight	702.18 g/mol
Space group	Monoclinic Cc
Unit cell length (Å)	a= 16.3336, b= 17.8055, c= 9.5656
Unit cell angle	α= 90°, β= 96.898°, ɣ= 90°
volume	2761.81 $Å^3$

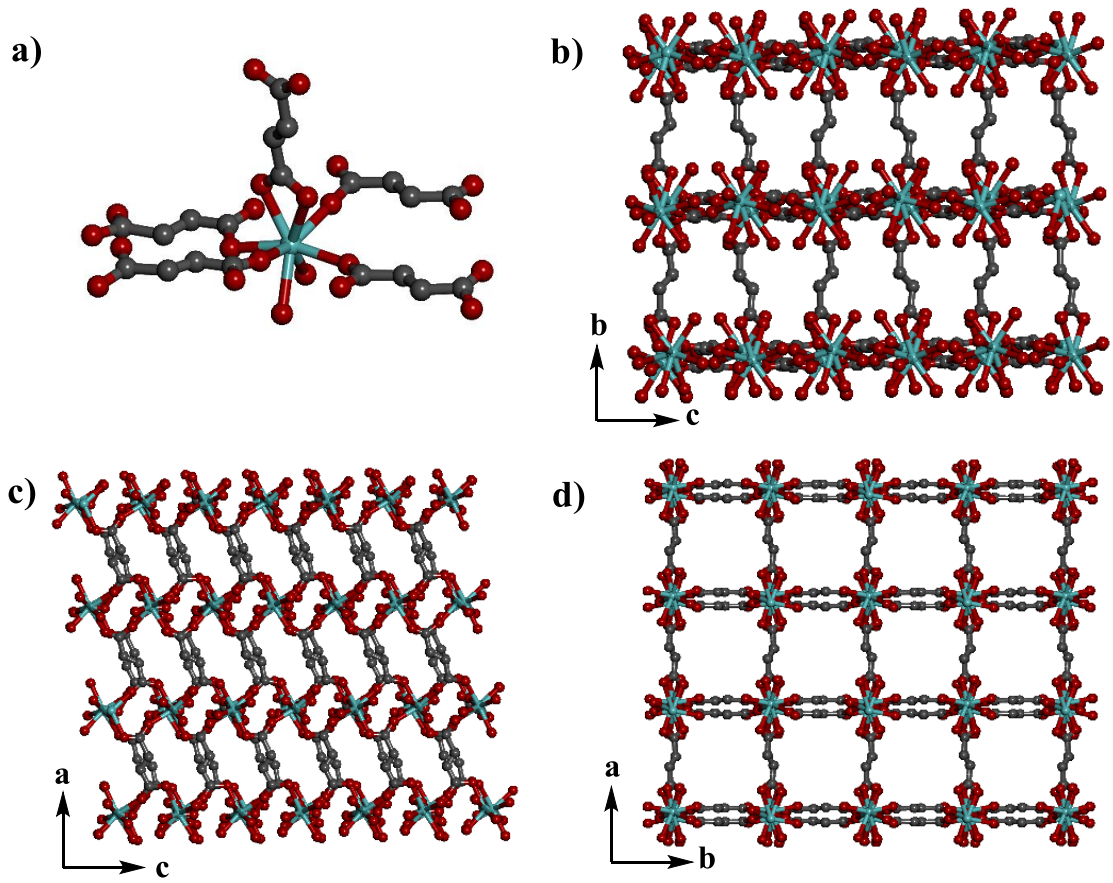

Figure 5: Single crystal structure: a) coordination of Yttrium in **2**, b) crystal structure view along a-axis, c) b-axis, d) c-axis of **2**(solvents in the pore are removed for clarity).[Blue-Yttrium, Grey-Carbon, Red-Oxygen].

The metal center i.e. yttrium is eight coordinated with four fumaric acid in a monodendate fashion and one fumaric acid in bidendate fashion and by two water molecules (fig 5a). The metal centers are connected by fumarate moieties to form a 3D extended framework which is 2D porous, along the a-axis and c-axis (fig 5). The pores are filled with two DMF molecules. PLATON analysis shows a void volume of

41%. The pore window along the a-axis is 12.081Å x 4.818Å and along the c-axis is 10.320 Å x 9.480Å.

3.2.4 Bulk characterization

Bulk characterization was performed using Powder X-ray diffraction (PXRD) and Thermogravimetric Analysis (TGA).

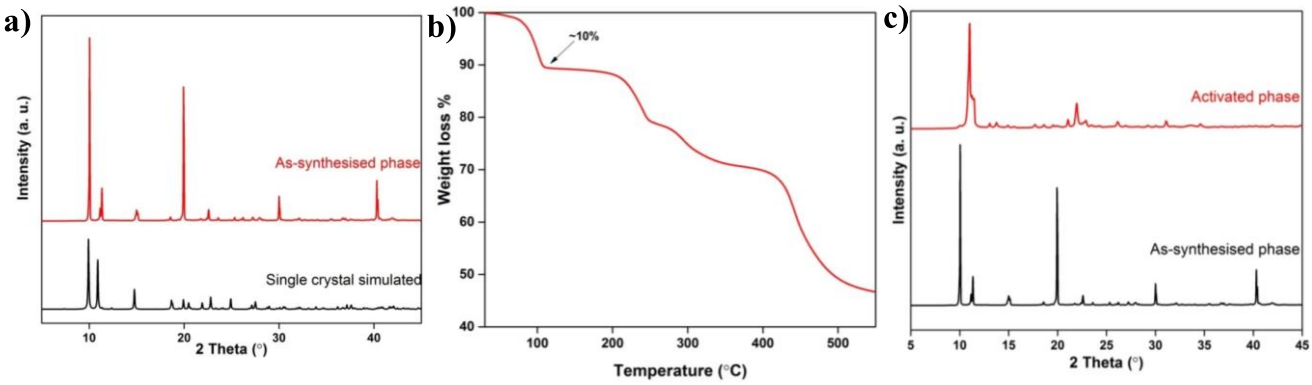

Figure 6: Bulk characterization: a) PXRD of as-synthesized and SC simulated phase of **2**, b) TGA of **2**, c) PXRD of activated phase **2**.

PXRD comparison of bulk and single crystal simulated phase shows that the phase obtained is pure. TGA reveals a weight loss of approximately 10% from 30°C to 100°C, which corresponds to the loss of one DMF molecule from the pore and the framework is stable up to 200°C. For checking the porosity of the sample, it was activated at 100°C for 6 hours under high vacuum (10^{-5}torr). The PXRD of activated sample shows a different phase (fig 6c), which is non-porous. Hence the MOF obtained here is a first generation MOF, where the framework collapses partially upon the removal of pore solvents and thus shows no porosity.

Chapter-4

CO_2 sorption studies on $Cu(INA)_2$ MOF.

4.1 Synthesis

4.1.1 Synthesis of $Cu(INA)_2$•MeOH(**3**)

3 was synthesized solvothermally, by heating 1mmol of $CuCl_2.2H_2O$ and 2mmol of HINA in 1:1 mixture of DMF and MeOH in a 20 ml Teflon liner at 90°C for 72hrs followed by slow cooling to room temperature over a period of 12 hrs. Blue long rod shaped crystals were isolated by filtration and washed with water and methanol. The air dried sample gave a total yield of 270mg.

4.1.2 Synthesis of $Cu(INA)_2$•EtOH(**4**)

4 was synthesized solvothermally, by heating 1 mmol of $CuCl_2.2H_2O$ and 2 mmol of HINA in 1:1 mixture of DMF and EtOH in a 20 ml Teflon liner at 100°C for 60 hrs followed by slow cooling to room temperature over a period of 12 hrs. Blue long rod shaped crystals were isolated by filtration and washed with water and methanol. The air dried sample gave a total yield of 185mg.

4.1.3 Synthesis of $Cu(INA)_2$•0.75PrOH (**5**)

5 was synthesized solvothermally, by heating 1 mmol of $CuCl_2.2H_2O$ and 2 mmol of HINA in 1:1 mixture of DMF and PrOH in a 20 ml Teflon liner at 100°C for 60 hrs followed by slow cooling to room temperature over a period of 12 hrs. Blue long rod shaped crystals were isolated by filtration and washed with water and methanol. The air dried sample gave yield of 190mg.

4.1.4 Synthesis of $Cu(INA)_2(H_2O)_2$ *(***6***)*

6was synthesized solvothermally, by heating 1 mmol of $CuCl_2.2H_2O$ and 2 mmol of HINA in 5 ml in a 20 ml Teflon liner at 90°C for 72hrs followed by slow cooling to room temperature over a period of 12 hrs. Blue block shaped crystals were isolated by filtration washed with water and methanol. The air dried sample gave yield of 165 mg.

4.2 Results and Discussion

4.2.1 Crystal structure description of 3, 4, 5 & 6

Table 3: Crystal structure description of **3** and **4**.

Sample	**3**	**4**
Empirical formula	$Cu(C_5H_4N)_2{\bullet}CH_4O$	$Cu(C_5H_4N)_2{\bullet}C_2H_6O$
Formula weight	251.77 g/mol	265.08 g/mol
Space group	Monoclinic Cc	Monoclinic Cc
Unit cell length(Å)	(4.87, 25.097, 10.782)	(5.03, 24.855, 11.176)
Unit cell angle	(90°, 96.82°, 90°)	(90°, 99.53°, 90°)
Volume (Å^3)	1308.55	1379.435

Table 4: Crystal description of **5** and **6**.

Sample	**5**	**6**
Empirical formula	$Cu(C_5H_4N)_2{\bullet}C_3H_8O$	$Cu(C_5H_4N)_2(H_2O)_2$
Formula weight	279.82 g/mol	255.76 g/mol
Space group	Monoclinic Cc	Triclinic P-1
Unit cell length(Å)	(5.165, 24.466, 11.585)	(6.31, 6.31, 9.2)
Unit cell angle	(90°, 101.56°, 90°)	(98.89°, 105.12°, 108.6°)
Volume (Å^3)	1434.159	349

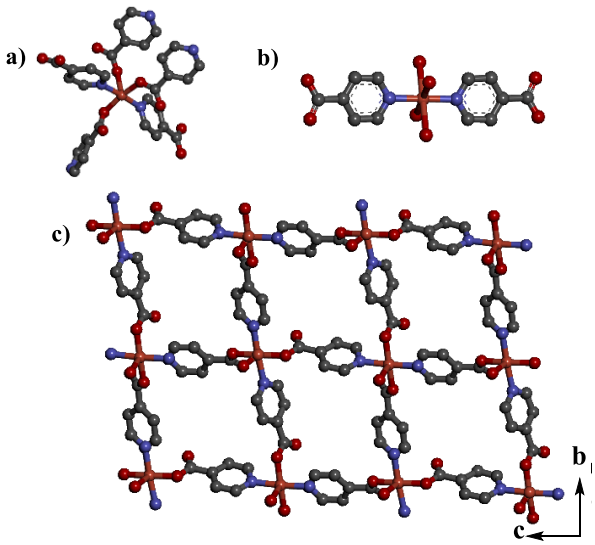

Figure 7: Single crystal structure: a) coordination of copper in **3.** b) Coordination of copper in **6**, c) Crystal structure view of **3** along a-axis.

In **3** the central copper atom is penta-coordinated. The coordinations are satisfied by two pyridyl groups of isonicotinic acid (INA) and two carboxylate group of INA binding in a monodendate fashion in the equatorial position and one carboxylate group of HINA coordinating in monodendate fashion in the axial position, to give square pyramidal geometry[42] (fig 7a).The monodendate isonicotinic acid binds to another copper center to form an extended 3D framework. The frameworks **3**, **4** and **5** are isostructural. On the other hand, **6** does not form an extended coordination network. Only nitrogen of two INA is coordinated to Cu center with four water molecules and the Cu center is six coordinated (fig 7b). Single crystal structure of **3** reveals that the framework is 3D with 1D porous channel along the a-axis. PLATON calculation gives a void volume of only 12% for the compound **3**.

The pore window along the a-axis is 7.838Å x 8.884Å (fig 8) excluding the Vander-Waal radii. There are two diagonal pore width 12.783Å and 10.783Å. Two different pore widths corresponds to the flexibility of the ligand. This monodendate binding of carboxylate group gives flexibility to the framework for the inclusion of polar solvents like methanol, ethanol and propanol.

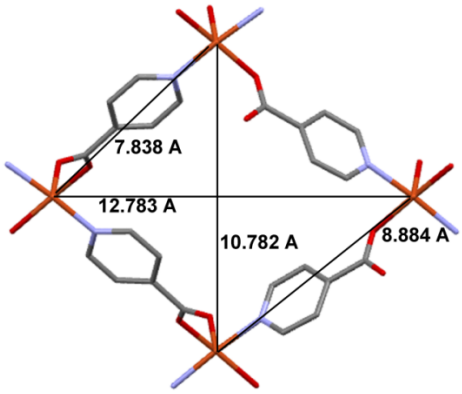

Figure 8: Pore window dimensions of **3** along the a-axis.

4.2.2Bulk characterization

PXRD, TGA and Adsorption have been performed for the bulk characterization of the material. PXRD of the bulk matches quiet well with that of the single crystal simulated XRD indicating the phase purity of the compounds (fig 9).

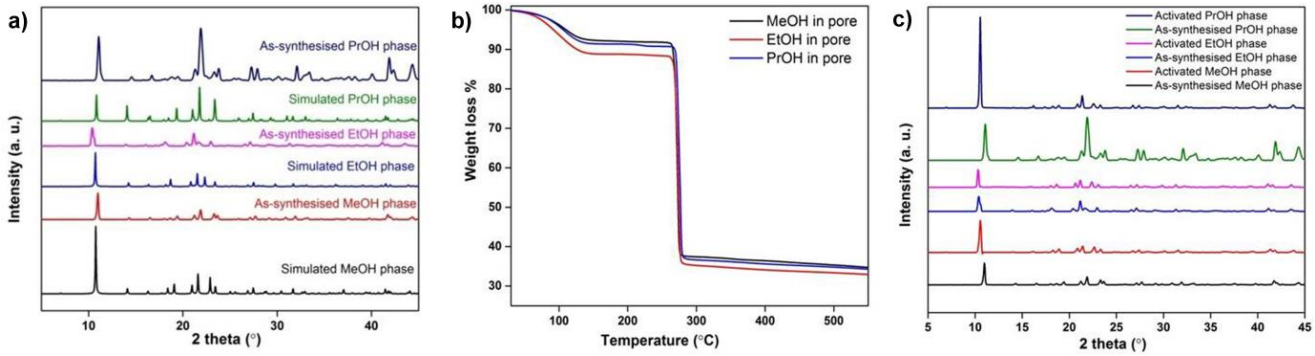

Figure 9: Bulk characterization: a) PXRD of **3**(MeOH), **4**(EtOH), **5**(PrOH) b) TGA of **3, 4** & **5**. c) PXRD of activated **3, 4** & **5**.

TGAs for all three phases show thermal stability up to 270°C. Crystal structure shows presence of one MeOH, one EtOH and 0.75 PrOH in the pore of the **3**, **4** and **5** respectively, which is also supported by TGA, which shows a weight loss of ~8.5% in case of **3** and **5**and a weight loss of ~12% in case of **4**, corresponding to the loss of these solvents from the pore.

3, 4 and **5** were activated at 180°C for 6hrs under high vacuum of 10^{-5}torr. PXRD of the activated sample shows that all three samples are extremely stable to the activation procedure. Lowering of intensity of some PXRD peaks in the as-synthesized phase in the activated sample might be due to solvent removal. All three activated phases are exactly the same.

4.2.3 CO_2 adsorption studies and selectivity to CO_2 over N_2 at room temperature.

Since **3**, **4** and **5** are isostructural, adsorption studies on EtOH phase (**4**) is mentioned for consistency. Prior to adsorption, sample **4** is activated at 180°C under 10^{-5} torr vacuum and evacuated at 180°C. Adsorption of CO_2 at 273K, 283K and 298K and N_2 at 298K has been performed. CO_2 isotherm is observed to be nearly type 1 isotherm, in which the CO_2 molecules are diffused into the pore with increase in pressure. It shows CO_2 uptake of 2.99 mmol/g at 273K and 2 mmol/g at 298K. At 298K, only 0.03mmol/g of N_2 is adsorbed in this material. This ensures that the MOF is apparently highly selective to CO_2/N_2 at room temperature (fig 10).

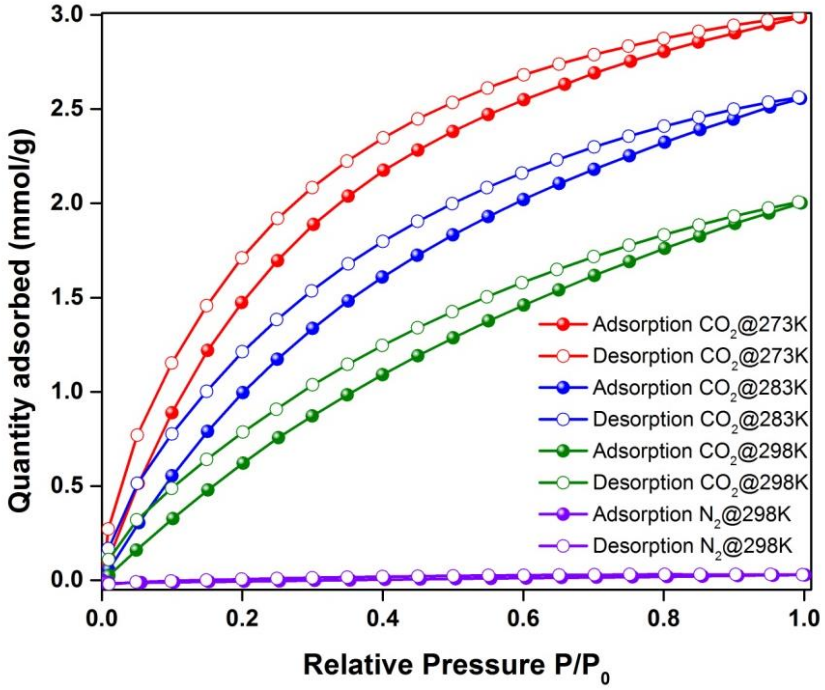

Figure 10: Adsorption isotherm of CO_2 at 273K, 283K, 298K and N_2 at 298K.

This material possesses a BET surface area of~250m^2/g and Langmuir surface area of ~515m^2/g (fig 11, table 5).

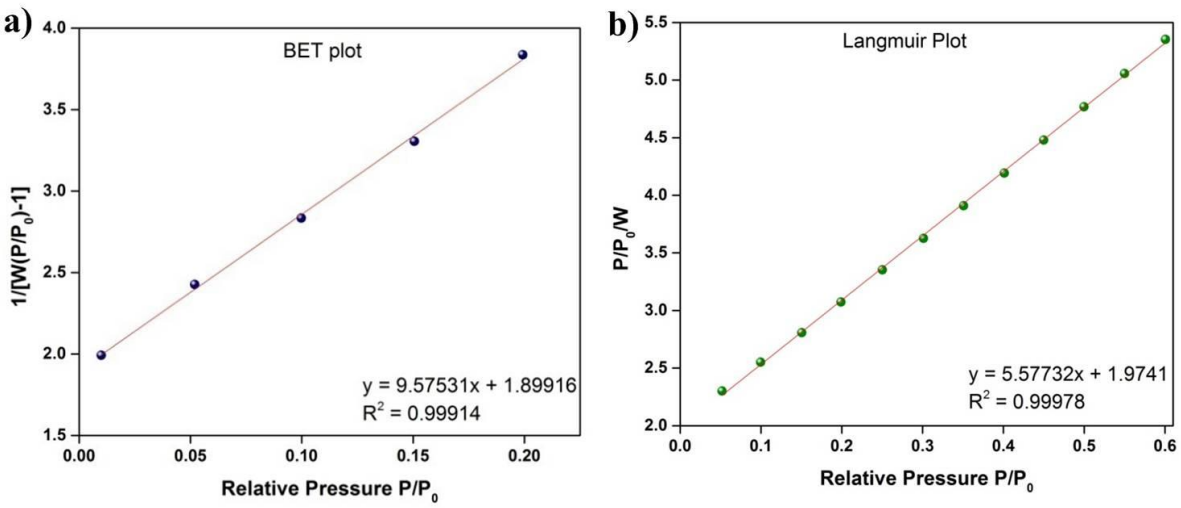

Figure 11: a) BET fit, b) Langmuir fit of compound **4**.

BET and Langmuir surface area were calculated from 273K CO_2 isotherm.

Table 5: Summary of BET and Langmuir plot.

	BET	Langmuir
Surface Area	250.429 m^2/g	515.212 m^2/g
Slope	9.57531 ±0.22966 g/mmol	5.57732± 0.0374 g/mmol
y-intercept	1.89916 ±0.0215 g/mmol	1.9741±0.0137 g/mmol
B		2.82524
C	6.042	
Wm	0.08714 mmol/g	0.1793 mmol/g

Non-Linear Density Function Theory (NLDFT) for pore size distribution:

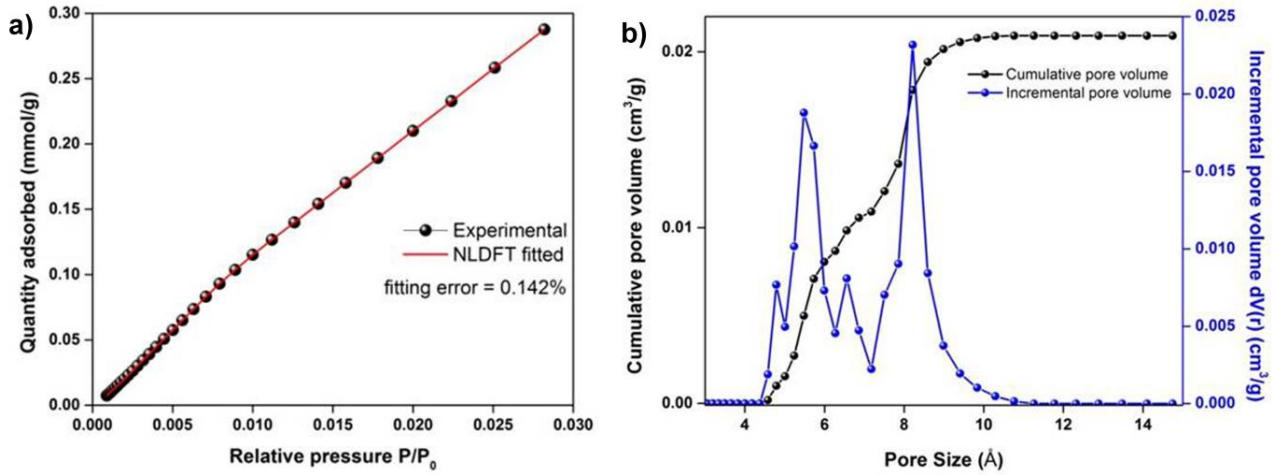

Figure 12: a) NLDFT fit of 273K CO_2 of **4,** b) Pore size distribution of compound **4**.

Non-Linear Density Function Theory (NLDFT) fitted isotherm and experimental isotherm of CO_2 at 273K fitted very well with an error of only 0.142% (fig 12a). This method reveals a pore size of 5.48 Å and 8.2 Å with pore volume of 0.016 cm^3/g and 0.021cm^3/g (fig 12 b) and a pore surface area of 62.47m^2/g. The pore size obtained is similar to the single crystal data if the Vander Waal radii is taken into consideration (fig 8). Two different pore width indicate the undulation motion of pore on CO_2 adsorption (i.e, one pore shrinks and other expands).

Heat of Adsorption for CO_2 from Virial Model:

The CO_2 adsorption was measured from 0- 1bar at 273, 283, 298 K and was fitted by virial equation, given below;

$$ln(P) = ln(Va) + (a0 + a1 * Va + a2 * Va\text{^}2 \ldots + a6 * Va\text{^}6)/T + (b0 + b1 * Va) \ldots\ldots\ldots$$

P is pressure, V_a is amount of CO_2 adsorbed, T is temperature and a0, a1, a2, a3, a4, a5, a6, b0, b1, b2, b3 are empirical parameters.

Table 6: Summary of the fitted virial parameters.

a0	-4290.42144
a1	923.296
a2	-166.3995
a3	2.2516
a4	6.96E-06
b0	20.3082
b1	-3.1976
b2	0.67679

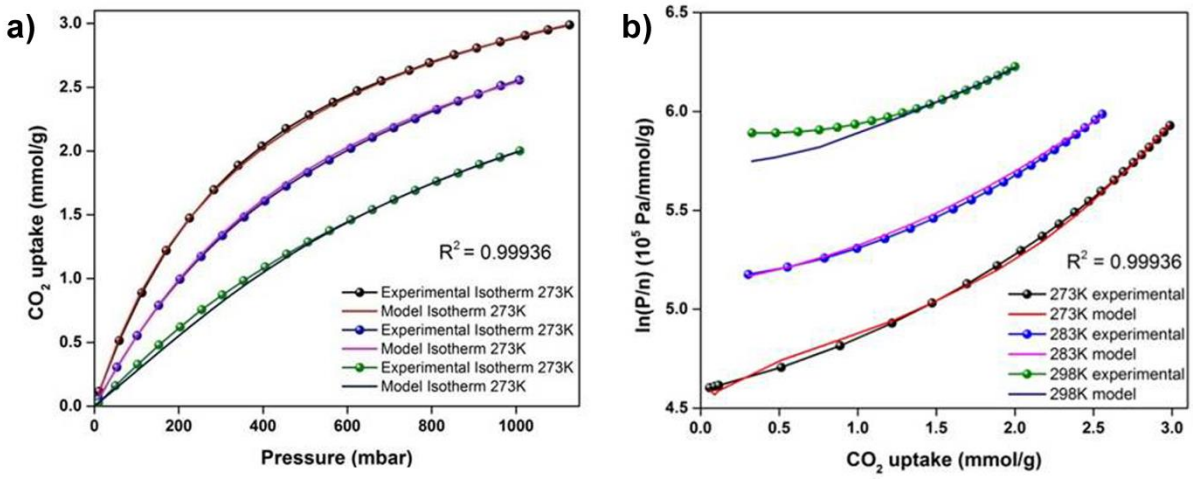

Figure 13: a) Fitting of experimental isotherm of CO_2 at 273K, 283K and 298K with the virial model, b) Virial plots carried out using CO_2 isotherms.

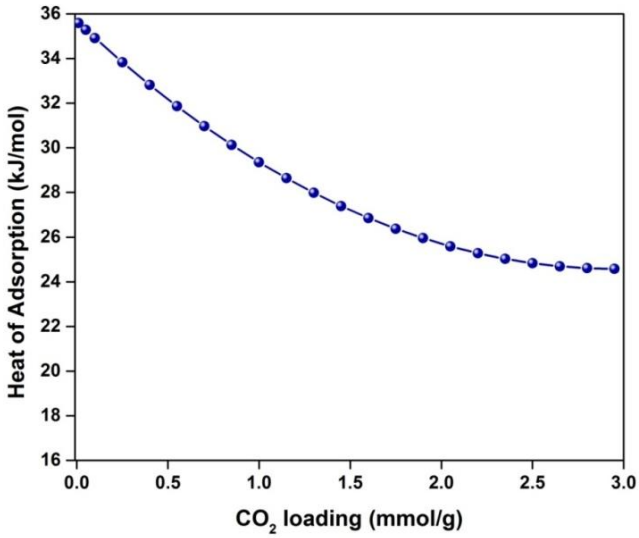

Figure 14: HOA calculated from virial modelling using CO_2 isotherm at 273K, 283K and 298K.

CO_2 adsorption at 273K, 283K and 298K were fitted with virial model (fig 13) with virial fitting parameters mentioned in table 6. HOA for CO_2 in this material is found to be 35.67kJ/mol, which is a moderate value. The HOA is observed to be decreasing with increasing CO_2 loading. At a high CO_2 loading of 2.95mmol/g, the HOA is found to be 24.64kJ/mol.

<u>CO_2/N_2 Selectivity using Ideal Adsorbed Solution Theory (IAST) modelling:</u>

The selectivity of gas is measured by this formula below.

$$S1,2 = (\frac{q1}{q2})/(\frac{P1}{P2})$$

$S_{1,2}$= Selectivity of gas 1over 2.

q_1 = quantity of gas 1 adsorbed, q_2 = quantity of gas 2 adsorbed.

P_1 = pressure at which gas 1 is adsorbed, P_2 = pressure at which gas 2 is adsorbed.

The post combustion flue gas has 0.15 bar partial pressure of CO_2 and 0.75 bar partial pressure of N_2.

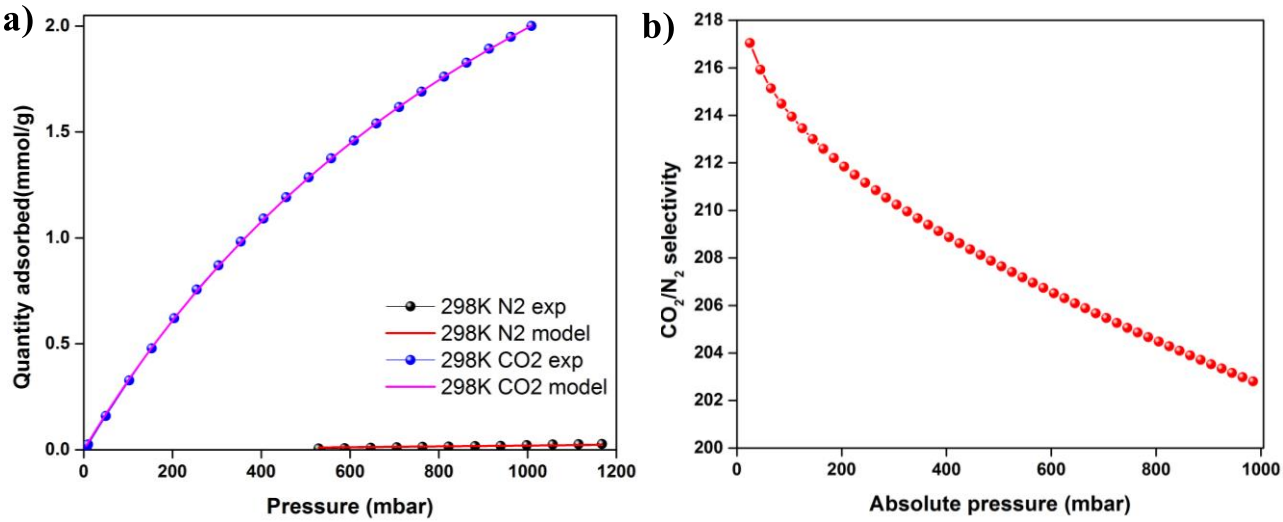

Figure 15: a) IAST fitting of 298K CO_2 and N_2, b) CO_2/N_2 selectivity calculated from IAST model.

CO_2 and N_2 at 298K were fitted with IAST model in order to obtain CO_2/N_2 selectivity (fig 15a).The isotherm fitted well with the Dual Site Langmuir (DSL) model of IAST. The selectivity value is approximately 217 at 25 mbar pressure and it decreases to approximately 203 at 1 bar pressure. Selectivity value highly depends on the low quantity of N_2 adsorbed compared with CO_2.

Table 7: Summary of results of framework **4**.

$Cu(INA)_2$	
BET surface area	~250 m^2/g
Langmuir surface area	~515 m^2/g
Pore size	5.48 Å & 8.2 Å
Cumulative pore volume	0.016 cm^3/g & 0.021 cm^3/g
Cumulative pore surface area	62.47 m^2/g
Heat of Adsorption	~36 kJ/mol
CO_2/N_2 selectivity	~217

Table 8: Comparison of 4 with some reported MOFs.

MOF name	CO_2 uptake at 0.15 bar (mmol/g)	N_2 uptake at 0.75 bar (mmol/g)	Selectivity	Temperature
$Zn_2(atz)_2(ox)$[28]	2.05	-		298K
Ni-4-PyC[24]	1.6	0.06	1853	313K
Mg-MOF-74[42]	5.87	0.66	232	303K
$Cu(INA)_2$ (**4**)	0.48	0.014	217	298K

Conclusion

Mitigation of atmospheric CO_2 concentrations is a key to addressing global warming created by this greenhouse gas. Pressure/Temperature swing adsorption process is identified as the best method for large scale CO_2 capture. Efficiency of this technology depends to a large extent on the CO_2 sorption-desorption dynamics of the sorbent materials. Ultra-microporous MOFs, if developed to have optimal capacity and selectivity for CO_2 over N_2, can serve as excellent sorbents for capturing CO_2 from flue gas, the major industrial effluent. For these post-combustion capture applications, which involve capturing CO_2 at low partial pressures, here we are making ultra-microporous MOFs with three-dimensional structure, by employing highly coordinating Yttrium as metal centre and rigidly chelating oxalate/fumarate as ligand. The Yttrium oxalate and fumarate frameworks developed here possesses large void volume of 39% and 41%. Despite the large coordination around Y and chelation by oxalate/fumarate, the frameworks collapse upon removal of the occluded solvents making the MOFs not suitable for gas capture. This makes them candidates representing first generation MOFs[43]. On the other hand, the $Cu(INA)_2$ prepared possess only 12% void volume and are second generation MOFs because they maintain their structural integrity upon removal of solvent. These MOFs are highly moisture stable and have a CO_2 uptake of 2.99 mmol/g at 273K and 2 mmol/g at 298K and 900 mmHg pressures. They are ultra-microporous with a pore size of 4-8 Å and Langmuir surface area of ~515m2/g. They possess high CO_2/N_2 selectivity at room temperature and 1 bar pressure, with a selectivity value of ~217. This selectivity value is close to that of the one of the top-performing Mg-MOF-74. The heat of adsorption for CO_2 in this material is ~35.67 kJ/mol at zero loading and it decreases as the CO_2 loading increases. We are presently developing the scale-up and further investigations on the CO_2 kinetics of this $Cu(INA)_2$ MOF and trying to come-up with alternate strategies to transform the first generation Yttrium MOFs into stable second generation ones.

References

(1) Rosi, N. L.; Eckert, J.; Eddaoudi, M.; Vodak, D. T.; Kim, J.; O'Keeffe, M.; Yaghi, O. M. *Science.* **2003**, *300* (5622), 1127-1129.

(2) Nugent, P.; Belmabkhout, Y.; Burd, S. D.; Cairns, A. J.; Luebke, R.; Forrest, K.; Pham, T.; Ma, S.; Space, B.; Wojtas, L.; Eddaoudi, M.; Zaworotko, M. J. *Nature* **2013**, *495* (7439), 80–84.

(3) Phan, A.; Czaja, A. U.; Gándara, F.; Knobler, C. B.; Yaghi, O. M. *Inorg. Chem.* **2011**, *50* (16), 7388–7390.

(4) Yoon, M.; Suh, K.; Natarajan, S.; Kim, K. *Angew. Chemie Int. Ed.* **2013**, *52* (10), 2688–2700.

(5) (Horcajada, P.; Chalati, T.; Serre, C.; Gillet, B.; Sebrie, C.; Baati, T.; Eubank, J. F.; Heurtaux, D.; Clayette, P.; Kreuz, C.; Chang, J.-S.; Hwang, Y. K.; Marsaud, V.; Bories, P.-N.; Cynober, L.; Gil, S.; Ferey, G.; Couvreur, P.; Gref, R. *Nat Mater* **2010**, *9* (2), 172–178.

(6) Chapman, M. E.; Ayyappan, P.; Foxman, B. M.; Yee, G. T.; Lin, W. *Cryst. Growth Des.* **2001**, *1* (2), 159–163.

(7) Rackley S. Carbon capture and storage. Burlington; MA: Butterworth-Heinemann/Elsevier; 2010.

(8) Eddaoudi, M.; Kim, J.; Rosi, N.; Vodak, D.; Wachter, J.; O'Keeffe, M.; Yaghi, O. M. *Science (80-.).* **2002**, *295* (5554), 469 LP-472.

(9) Granite, E. J.; Pennline, H. W. *Ind. Eng. Chem. Res.* **2002**, *41* (22), 5470–5476.

(10) Sumida, K.; Rogow, D. L.; Mason, J. A.; McDonald, T. M.; Bloch, E. D.; Herm, Z. R.; Bae, T.-H.; Long, J. R. *Chem. Rev.* **2012**, *112* (2), 724–781.

(11) Eirik .F.da Silvaa; Hallvard; Svendsena, F.; *Int. J. Greenhouse Gas Control,* **2007**,*1*,151-157.

(12) Rochelle, G. T. *Science (80-.).* **2009**, *325* (5948), 1652 LP-1654.

(13) Himeno, S.; Tomita, T.; Suzuki, K.; Yoshida, S. *Microporous Mesoporous Mater.* **2007**, *98* (1), 62–69.

(14) Lee, J.-S.; Kim, J.-H.; Kim, J.-T.; Suh, J.-K.; Lee, J.-M.; Lee, C.-H. *J. Chem. Eng. Data* **2002**, *47* (5), 1237–1242.

(15) Wang, Y.; LeVan, M. D. *J. Chem. Eng. Data* **2009**, *54* (10), 2839–2844.

(16) Li, G.; Xiao, P.; Webley, P.; Zhang, J.; Singh, R.; Marshall, M. *Adsorption* **2008**, *14* (2), 415–422.

(17) Konduru, N.; Lindner, P.; Assaf-Anid, N. M. *AIChE J.* **2007**, *53* (12), 3137–3143.

(18) Choi, S.; Drese, J. H.; Jones, C. W. *ChemSusChem* **2009**, *2* (9), 796–854.

(19) Plaza, M. G.; García, S.; Rubiera, F.; Pis, J. J.; Pevida, C. *Chem. Eng. J.* **2010**, *163* (1–2), 41–47.

(20) Li, H.; Eddaoudi, M.; Groy, T. L.; Yaghi, O. M. *J. Am. Chem. Soc.* **1998**, *120* (33), 8571–8572.

(21) Millward, A. R.; Yaghi, O. M. *J. Am. Chem. Soc.* **2005**, *127* (51), 17998–17999.

(22) Furukawa, H.; Ko, N.; Go, Y. B.; Aratani, N.; Choi, S. B.; Choi, E.; Yazaydin, A. Ö.; Snurr, R. Q.; O'Keeffe, M.; Kim, J.; Yaghi, O. M. *Science (80-.).* **2010**, *329* (5990), 424 LP-428.

(23) Furukawa, H.; Cordova, K. E.; O'Keeffe, M.; Yaghi, O. M. *Science (80-.).* **2013**, *341* (6149).

(24) Nandi, S.; Collins, S.; Chakraborty, D.; Banerjee, D.; Thallapally, P. K.; Woo, T. K.; Vaidhyanathan, R. *J. Am. Chem. Soc.* **2017**, *139* (5), 1734–1737.

(25) Arstad, B.; Fjellvåg, H.; Kongshaug, K. O.; Swang, O.; Blom, R. *Adsorption* **2008**, *14* (6), 755–762.

(26) Vaidhyanathan, R.; Iremonger, S. S.; Shimizu, G. K. H.; Boyd, P. G.; Alavi, S.; Woo, T. K. *Science (80-.).* **2010**, *330* (6004), 650 LP-653.

(27) Vaidhyanathan, R.; Iremonger, S. S.; Dawson, K. W.; Shimizu, G. K. H. *Chem. Commun.* **2009**, No. 35, 5230–5232.

(28) Vaidhyanathan, R.; Iremonger, S. S.; Shimizu, G. K. H.; Boyd, P. G.; Alavi, S.; Woo, T. K. *Angew. Chemie Int. Ed.* **2012**, *51* (8), 1826–1829.

(29) Banerjee, A.; Nandi, S.; Nasa, P.; Vaidhyanathan, R. *Chem. Commun.* **2016**, *52* (9), 1851–1854.

(30) Iremonger, S. S.; Vaidhyanathan, R.; Mah, R. K.; Shimizu, G. K. H. *Inorg. Chem.* **2013**, *52* (8), 4124–4126.

(31) Aprea, P.; Caputo, D.; Gargiulo, N.; Iucolano, F.; Pepe, F. *J. Chem. Eng. Data* **2010**, *55* (9), 3655–3661.

(32) Choi, S. B.; Seo, M. J.; Cho, M.; Kim, Y.; Jin, M. K.; Jung, D.-Y.; Choi, J.-S.; Ahn, W.-S.; Rowsell, J. L. C.; Kim, J. *Cryst. Growth Des.* **2007**, *7* (11), 2290–2293.

(33) Caskey, S. R.; Wong-Foy, A. G.; Matzger, A. J. *J. Am. Chem. Soc.* **2008**, *130* (33), 10870–10871.

(34) Mason, J. A.; Sumida, K.; Herm, Z. R.; Krishna, R.; Long, J. R. *Energy Environ. Sci.* **2011**, *4* (8), 3030–3040.

(35) Li, Y.; Yang, R. T. *Langmuir* **2007**, *23* (26), 12937–12944.

(36) Demessence, A.; D'Alessandro, D. M.; Foo, M. L.; Long, J. R. *J. Am. Chem. Soc.* **2009**, *131* (25), 8784–8786.

(37) Furukawa, H.; Gándara, F.; Zhang, Y.-B.; Jiang, J.; Queen, W. L.; Hudson, M. R.; Yaghi, O. M. *J. Am. Chem. Soc.* **2014**, *136* (11), 4369–4381.

(38) Nandi, S.; De Luna, P.; Daff, T. D.; Rother, J.; Liu, M.; Buchanan, W.; Hawari, A. I.; Woo, T. K.; Vaidhyanathan, R. *Sci. Adv.* **2015**, *1* (11).

(39) Lu, T.-B.; Luck, R. L. *Inorganica Chim. Acta* **2003**, *351*, 345–355.

(40) Lu, J. Y.; Babb, A. M. *Chem. Commun.* **2002**, No. 13, 1340–1341..

(41) S. Maurer, Prediction of Single Component Adsorption Equilibria*, Herbert Utz Publisher,* **2000,** 2000-2232.

(42) Zhang, Z.; Yao, Z.-Z.; Xiang, S.; Chen, B. *Energy Environ. Sci.* **2014**, *7* (9), 2868–2899.

(43) Kitagawa, S.; Uemura, K. *Chem. Soc. Rev.* **2005**, *34* (2), 109–119.